Microbiome

RESEARCH Open Access

Granular activated carbon (GAC)-driven microbial electron shuttle boosts denitrification and mitigates N_2O in cold and carbon-limited biofilm system

Xiangyu Yang[1,2,3,4†], Mingchen Yao[1,4,5†], Peng Li[6], Jan Peter van der Hoek[4,7], Lujing Zhang[4,6] and Gang Liu[1,4,5*]

Abstract

Background Denitrification in wastewater treatment is severely limited under low-temperature and low-carbon ("dual-low") conditions, hindering sustainable nitrogen removal. Biofilm systems, though energy-efficient, suffer from reduced efficiency in such environments due to impaired interspecies electron transfer (IET). Granular activated carbon (GAC), a conductive mediator, offers potential to enhance IET between electroactive microorganisms (EAMs) and denitrifiers, yet its role in dual-low systems remains underexplored. This study investigates GAC's capacity to optimize biofilm functionality and mitigate greenhouse gas (GHG) emissions under these constraints.

Results Under dual-low conditions (4–6°C, C/N = 4), GAC increased denitrification efficiency by 19.4–21.9% and reduced N_2O emissions by 10.6–22.9%. Metatranscriptomes revealed upregulation of denitrifying genes (e.g., *nosZ*) and electron transport pathways (e.g., *omc*B in *Geobacter*). FISH/SEM confirmed GAC-driven coacervates of EAMs and denitrifiers, linked by nanowires, enhancing direct electron transfer. Microbial diversity decreased, but functional redundancy improved, with *Pseudomonas fluorescens* and *Geobacter sulfurreducens* dominating. TOC removal rose under low temperatures, indicating enhanced carbon utilization.

Conclusions GAC fosters synergistic EAM-denitrifier partnerships, enabling efficient denitrification and GHG mitigation in cold and carbon-limited ("dual-low") biofilm systems, advancing sustainable wastewater management.

Keywords Biofilm, Denitrification, Low-temperature/carbon source, Granular activated carbon, Electron transfer

†Xiangyu Yang and Mingchen Yao are co-first author.

*Correspondence:
Gang Liu
gliu@rcees.ac.cn; g.liu-1@tudelft.nl
[1] Key Laboratory of Environmental Aquatic Chemistry, State Key Laboratory of Regional Environment and Sustainability, Research Centre for Eco-Environmental Sciences, Chinese Academy of Sciences, Beijing 100085, P. R. China
[2] Key Laboratory of Marine Environment and Ecology, Ministry of Education, College of Environmental Science and Engineering, Ocean University of China, Qingdao 266100, P. R. China
[3] Shandong Provincial Key Laboratory of Marine Environment and Geological Engineering (MEGE), College of Environmental Science and Engineering, Ocean University of China, 238 Songling Road, Qingdao 266100, P. R. China
[4] Section of Sanitary Engineering, Department of Water Management, Faculty of Civil Engineering and Geosciences, Delft University of Technology, Delft 2628 CN, The Netherlands
[5] University of Chinese Academy of Sciences, Beijing 100049, P. R. China
[6] China Water Environment Group, Beijing 101101, P. R. China
[7] Department Research & Innovation, Waternet, Amsterdam 1090 GJ, The Netherlands

Introduction

In our rapidly developing society, rising food and energy consumption has led to increased reactive nitrogen (RN) generation [1], causing unintended consequences such as air and water pollution, soil acidification, biodiversity loss, and global warming [2–4]. However, addressing RN pollution—arising from various sources (e.g., farmland, livestock, wastewater) and in multiple forms (e.g., ammonia (NH_4^+), nitrate (NO_3^-), nitrous oxide (N_2O))—remains a significant challenge. Halving nitrogen waste is crucial for achieving Sustainable Development Goals (SDGs) in the coming decades. The United Nations Environment Programme (UNEP) has set a global target to cut nitrogen waste in half to support SDGs, including clean water (SDG 6) and climate action (SDG 14) [5, 6]. Advanced wastewater treatment technologies and management strategies are essential for reducing dissolved RN (primarily NO_3^-) discharge into aquatic environments. However, these solutions often involve high energy consumption and carbon emissions [7, 8], especially under low-temperature and low-carbon ("dual-low") conditions [9, 10]. Developing energy-efficient, low-carbon methods for RN removal in municipal wastewater treatment plants (WWTPs) is therefore a critical challenge worldwide.

Biofilm technology is an efficient, energy-saving, and environmentally friendly wastewater treatment method [11] that has gained significant attention, particularly in the context of the global "carbon neutral" initiative [12, 13]. Biofilm systems offer high microbial density, short hydraulic retention time (HRT), and low operational energy consumption [14, 15]. They also support a well-established denitrifier community capable of efficiently converting NO_3^- [11, 16]. Additionally, biofilm systems generate minimal sludge, reducing energy demands for sludge transportation and treatment in WWTPs [17]. However, their denitrification efficiency—especially in biofilters and constructed wetlands—declines sharply under "dual-low" conditions, limiting their widespread application.

Biofilm systems host a diverse microbial community, including denitrifiers and gram-negative electroactive microorganisms (EAMs) such as *Geobacter*, *Shewanella*, and *Rhodoferax* [18], which comprise 13–16% of the total microbial abundance in wastewater treatment system [19, 20]. Notably, EAMs can facilitate NO_3^- reduction by transferring electrons to denitrifiers either directly via nanowires or indirectly via electron shuttles [21]. Studies have shown that *Geobacter sulfurreducens*, a model EAM strain, exhibits cold resistance and can sustain respiration at temperatures as low as 4–15°C [22, 23]. Building on this, we propose enriching EAMs to enhance carbon source utilization and stimulate denitrifiers metabolism through interspecies electron transfer (IET) under "dual-low" conditions, thereby improving denitrification efficiency. However, increasing EAM abundance and activity in biofilm systems remains a significant challenge.

Studies have shown that EAMs transfer electrons to external electron acceptors, such as oxygen, oxidized compounds, and conductive materials, releasing energy as adenosine triphosphate (ATP) to support various life activities [24–27]. Existing strategies for enriching EAMs primarily focus on enhancing IET from the cytoplasm to flagella and external acceptors [28–30]. In this process, quinone-based electron shuttles can further facilitate IET between flagella and electron acceptors [31, 32]. Granular activated carbon (GAC), an effective electron mediator, possesses excellent electron storage and transfer capabilities, enabling membrane electrons to move to external media or microorganisms [33]. These mediators play a crucial role in enhancing EAM activity and abundance by promoting electron detachment in intracellular and membrane regions [26, 28]. Efficient electron transfer to denitrifiers can, in turn, improve the denitrification process.

Given abovementioned technological gaps and theoretical foundations, we used GAC as interventions to design a microcosmic biofilm model system. Our study aimed to improve denitrification efficiency and control greenhouse gas emission, investigated changes in biofilm structure and function, assessed the abundance and activity of EAMs and denitrifiers, and explored carbon source co-metabolism and IET processes in the biofilm system. Ultimately, it was expected to establish a tuning strategy for effective nitrogen reduction and removal in "dual-low" wastewater by biofilm systems.

Materials and methods

Experimental design and procedures

Set-up of biofilm model systems

We prepared 24 microcosm systems (two temperatures × two C/N ratios × two treatments × three replicates). Four treatments included control ("CK") and GAC ("G") treatments, respectively, and the control group (CK) used only ceramsite (*Φ*, 2–3 mm) as the biofilm carrier in 250-mL serum bottles with rubber stopper, while the GAC-treated group used a mixture of ceramsite and GAC (*Φ*, 2–3 mm) at a 3:1 of volume ratio to introduce conductive surfaces for potential electron transfer enhancement [26]. Half of the serum bottles were placed in the incubator at 25 ± 1°C (normal temperature, "N"), and the remaining bottles were kept at 4–6°C (cool temperature, "C"). The schematic diagram that visually summarizes the incubation biofilm system was showed in Supplementary Materials (Figure S1). The seeding sludge was acclimated for 3 months using synthetic

wastewater in batch mode (hydraulic retention time is 3 days). The process of biofilm growth was approximately for 3 months until the denitrifying efficiency was stable. Detailed methods of set-up are provided in Supplementary Materials (Text S1).

Preparation of synthetic wastewater

To simulate the variations of nitrogen and carbon sources in raw wastewater, the C/N ratios in synthetic wastewater were set at 8 and 4 by adjusting total organic carbon (TOC) levels. Detailed compositions of synthetic wastewater were approximately 400 mg/L TOC (C/N (TOC/NO_3^--N) = 8, shortly named as "H") and 200 mg/L TOC (C/N = 4, "L"), 50 mg/L nitrate (NO_3^--N), and 5 mg/L total phosphorus (TP). The initial pH of synthetic wastewater was adjusted to 7.0 by titrating with 4 M NaOH and 4 M HCl solutions, and the detail profile is provided in the Supplementary Materials (Text S2). All of the biofilm systems were named according to experimental conditions. For example, "CLCK" is that control group is under low temperature (C) and low carbon source (L) conditions.

Collection and detection of water and gas samples

We firstly conducted the enhanced experiment for 5 batches (15 days) and collected water samples at the end of each batch from each bottle at a half of the water level using a syringe for the analysis of water quality. And then, during the sixth batch considered as a typical batch, water samples were taken from each bottle at 0, 2, 4, 8, 12, 18, 24, 36, 48, 60, and 72 h to determine the kinetic trend of denitrification in one batch after enhancing experiment. The water samples were immediately store under − 20°C until analysis using a segmented flow analyzer (SAN + +, SKALAR, Netherlands). At the end of each batch, the headspace gas samples were undertaken by a syringe driven by the inter-pressure and stored in the 10 mL of the gas-sampling bags. The gas samples were measured using the gas chromatography (Shimadzu, GC-2010Plus, Japan) [34].

Biofilm morphology

After the formal experiment, ceramsite and GAC covered by biofilm were sampled from each microcosm for observing biofilm morphology and the spatial organization of EAMs and denitrifiers [35, 36]. The brief procedure of SEM was as follows: ceramsites and GAC were washed 3 times with the phosphate buffer and fixed with 2.5% glutaraldehyde. Subsequently, ceramsites and GAC were dehydrated and dried thoroughly. The dried biofilm was coated with gold and imaged using the field-emission SEM (FEI Quattro S, USA). The detailed profile is provided in the Supplementary Materials (Text S3).

Fluorescence in situ hybridization (FISH) analysis was referenced to previous study [37]. Briefly, ceramsites and GAC were fixed by the formaldehyde solution and followed by a double wash with ethanol. The washed biofilm was loaded into a 96-well plate for incubation and dehydration. Then, the plates were loaded with prepared hybridization buffer for hybridization. Oligonucleotide probes for FISH were designed specifically for targeted bacteria cells with (EAMs: 5′-GAAGACAGGAGGCCC GAAA-3′ labeled with CY5 [38] and denitrifiers: 5′-ACC CATGCATTTTCTTCCCGG-3′ labeled with 6-FAM) [39] and used for microscopic identification of the filamentous EAMs and spherical denitrifiers by FISH. The plates were examined using the confocal laser scanning microscope (CLSM, Leica, TCS SP8 CSU, Germany). The detail profile is provided in the Supplementary Materials (Text S3).

Biofilm response assay

The ATP concentrations, as a measure for microbial activity, were determined for all treatment groups. The total ATP concentration was determined, as described previously, using the Water-Glo™ reagent and a luminometer (Promega, USA) [40]. Electron transfer efficiency (ETE) was thus measured in this study through an electron respiration approach by reducing tetrazolium chloride to formazan [41, 42]. To monitor the long-range electrical fluctuation in biofilm as a function of space and time exposing to the enhancing materials, we measured the electrical signaling by using the fluorescent cationic dye thioflavin T (Th.T) to quantify the biofilm potential. The detailed methods were slightly modified according to the previous study [43], and data analysis is described in the Supplementary Materials (Text S4).

Analysis of microbial activity

At the end of first, third, and fifth batch, ceramsites and GAC covered by biofilm were collected from each microcosm for microbial activity analysis. Triplicate depths (top, middle, and below) of each bottle were randomly sampled and homogenized to get the biofilm [41]. The biofilm was stored at − 80°C until total DNA and RNA extraction. All raw data for the 16S rRNA gene and metatranscriptomes analyses have been deposited in the NCBI Sequence Read Archive (SRA) under accession number PRJNA995884.

Assembly sequencing

Total of DNA was extracted from each biofilm sample using the FastDNA SPIN kit (MP Biomedicals, Solon, OH, USA) following the manufacturer's instructions. Then, the duplicate DNA extracts were pooled for each sample and V4–V5 regions of prokaryotic 16S rRNA

genes were amplified using the primers 515F (5′-GTG YCAGCMGCCGCGGTAA-3′) and 926R (5′-CCGYCA ATTYMTTTRAGTTT-3′) by an ABI GeneAmp® 9700 PCR thermocycler (ABI, CA, USA). In this study, we only used short-read amplicons for annotation to illustrate trends in microbial community shifts; they reflect putative assignments based on best-hit matches and are primarily used to support functional interpretations in combination with metatranscriptomes data. The PCR amplification of 16S rRNA gene and the purification of pooled PCR products were performed in our previous study [44]. The details are shown in the Supplementary Materials (Text S5).

Metatranscriptomes analysis

Total of RNA were extracted from biofilm samples using the E.Z.N.A.® Soil RNA Midi Kit (Omega Biotek, Norcross, GA, USA) according to manufacturer's protocols. The RNA concentration and purity was quantified with NanoDrop2000 (Thermo Fisher Scientific, USA). The processes of RNA quality, rRNA removal, cDNA library construction, and transgenomics sequencing are described in the Supplementary Materials (Text S6).

Statistical analysis

In this study, the significance analyses of the data were performed using IBM SPSS (Version 22.0). The significant differences of parameters in different groups were tested with one-way ANOVA method followed by a post hoc Tukey test. The alpha- and beta-diversity analysis, non-metric multidimensional scaling (NMDS), and Kruskal–Wallis tests were performed using R packages (phyloseq, ampvis2, and vegan) [45]. The relative abundance of each enzymatic gene was the percentage of its predicted sequence number in total sequence number in one sample. Co-occurrence network analysis was conducted using the "Co-occurrence_network.R" script of MbioAssy1.0 (https://github.com/emblab-westlake/MbioAssy1.0) by analyzing all strong pairwise correlations between ASVs (Spearman's $\rho > 0.8$ and $P < 0.01$) that occurred in at least 50% of the samples [46].

Results

Composition and function of biofilm system

EAMs and denitrifiers enriched in biofilm system

To confirm the increase in abundance and activity of denitrifiers and EAMs, the FISH experiment was conducted, labeling EAMs and denitrifiers (Fig. 1). Under normal temperature and carbon conditions, the control

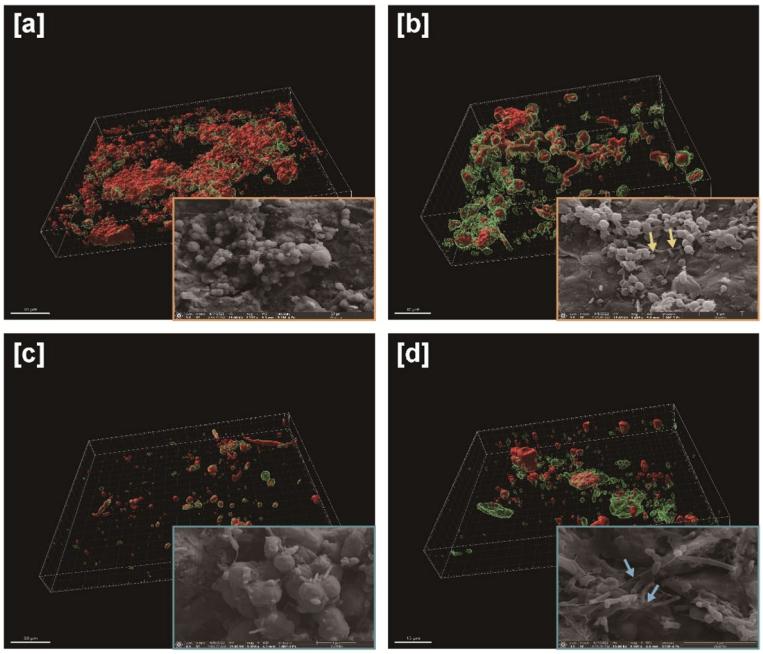

Fig. 1 Morphology images of microbial aggregates of EAMs and denitrifiers in the biofilm system by confocal laser scanning microscopy (CLSM) and scanning electron microscope (SEM) observation. **a**–**b** and **c**–**d** are under "double-normal" and "double-low" conditions, in which **a** and **c** are from the control group without the enhancement treatment, and **b** and **d** are from the GAC group. The colors in CLSM images indicate the fluorescence in situ hybridization (FISH) signals, and green and red represent EABs and denitrifiers, respectively. Arrows in SEM images highlight filamentous structures connecting bacterial cells, which are speculated to be microbial nanowires involved in interspecies electron transfer. Their identification is tentative and based on spatial organization, not direct molecular evidence

group had higher denitrifier abundance, while EAMs were scarce. In contrast, GAC group showed significantly increased EAMs signal density, forming coacervates with denitrifiers (EAMs cover the outside of denitrifiers in biofilm due to the supply and demand for electrons, which is so-called microbial chemotactic enrichment). Under "dual-low" conditions, control biofilms were sparse, but treatments enriched EAMs, increasing denitrifier signal density. Despite differences in abundance under "dual-low" conditions, bacterial clusters had similar compositions. SEM images revealed bacterial filaments connecting EAMs and denitrifiers, speculated to be nanowires facilitating the IET process. These processes likely promoted denitrifier activity and enhanced denitrification efficiency.

Furthermore, as shown in Figure S2, based on the in situ fluorescence imaging, results show that the biofilm composition and distribution on ceramsite and GAC carriers exhibited distinct differences, supporting the findings abovementioned. On the ceramsite surface (CK group), biofilms showed moderate and evenly distributed fluorescence intensities of total proteins, α-/β-polysaccharides, and lipids, indicating a stable but loosely structured biofilm layer. In contrast, GAC-supported biofilms displayed significantly stronger fluorescence signals, particularly for β-polysaccharides and lipids, suggesting a denser and more robust matrix structure. The high β-polysaccharide content is indicative of enhanced microbe–microbe and microbe–substrate bridging, which reinforces biofilm integrity and electron transfer networks. Additionally, elevated lipid and protein levels imply active microbial metabolism and extracellular polymer secretion. These observations corroborate the hypothesis that GAC fosters closer electroactive microbial–denitrifier interactions and stabilizes biofilm morphology through conductive bridging and enriched EPS production. Ultimately, this enhanced structural microenvironment may contribute to the improved denitrification efficiency and N_2O mitigation observed in GAC-amended systems under dual-low conditions.

Microbial activity in biofilm system

Microbial activity and electron transfer efficiency in the biofilm were tested, confirming the enhanced activity under treatment strategies compared to the control. Under "dual-low" conditions, ATP differences among treatments were insignificant; under low temperature and normal carbon, GAC treatment showed slightly higher ATP levels (increasing with 3.1%) (Fig. 2a). ETE testing showed all treatments significantly promoted ETE, consistent with increased microbial activity. Under "dual-low" conditions, GAC exhibited the highest increase 55.4%; Under normal temperature and low carbon, GAC group increased ETE to 70.6% with low carbon. Under double normal conditions, GAC increased with about 50% of ETE (Fig. 2a). To further assess the effect of the GAC treatment strategies on the biofilm system, biofilm potential was measured (Fig. 2b). Under "dual-low" conditions, control group biofilm potential fluctuated weakly, while GAC enhanced it, with higher

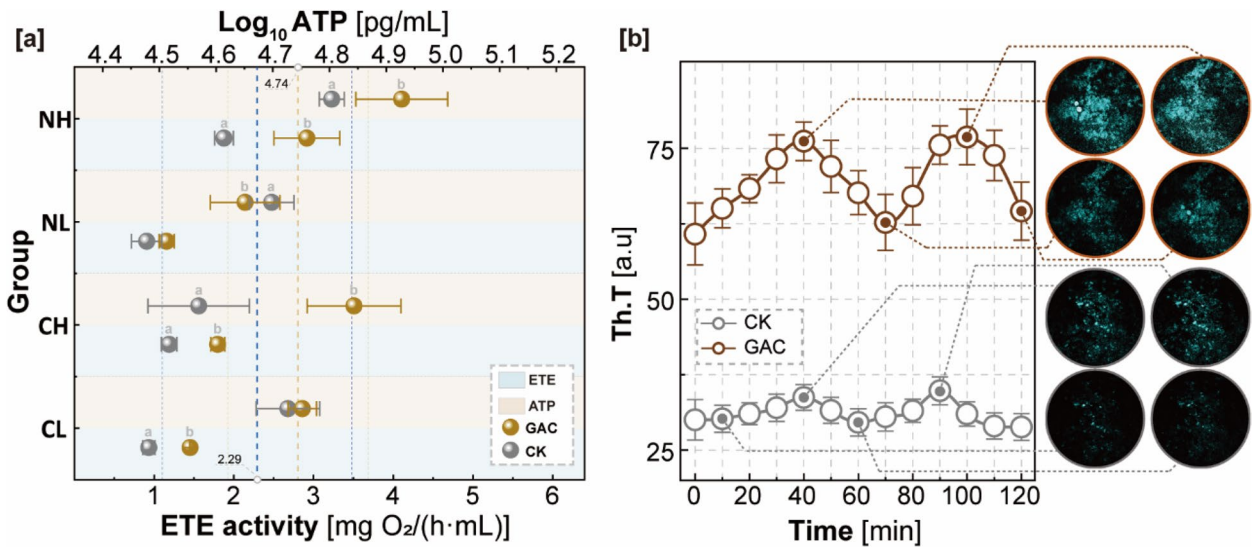

Fig. 2 **a** The activity of microorganisms in the biofilm system represented by ATP concentration and the electron transfer efficiency (ETE) of the whole biofilm system. **b** The fluctuation of signal changes of membrane potential of biofilm system under different treatment strategies (the fluorescence intensities are represented by the values and images, respectively.). Data are presented as the mean ± standard deviation, $n = 3$. Different letters indicate significant differences ($P < 0.05$) from the control

average signal intensities. Biofilm potential results were consistent with ETE, indicating that microbial activity and ETE were enhanced.

Reshaping of EAMs and denitrifiers community in biofilm

The microbial community structure in biofilm systems under "dual-low" condition differed significantly from "double-normal" ones (PERMANOVA, $P < 0.001$). GAC treatment strategy reduced microbial diversity and richness (Fig. 3a). NMDS analysis showed distinct community structure differences under the different treatments (Fig. 3b). GAC treatment had the most significant impact on community structure ($R^2 = 0.054$), indicating deterministic selection factors reducing microbiota diversity and richness.

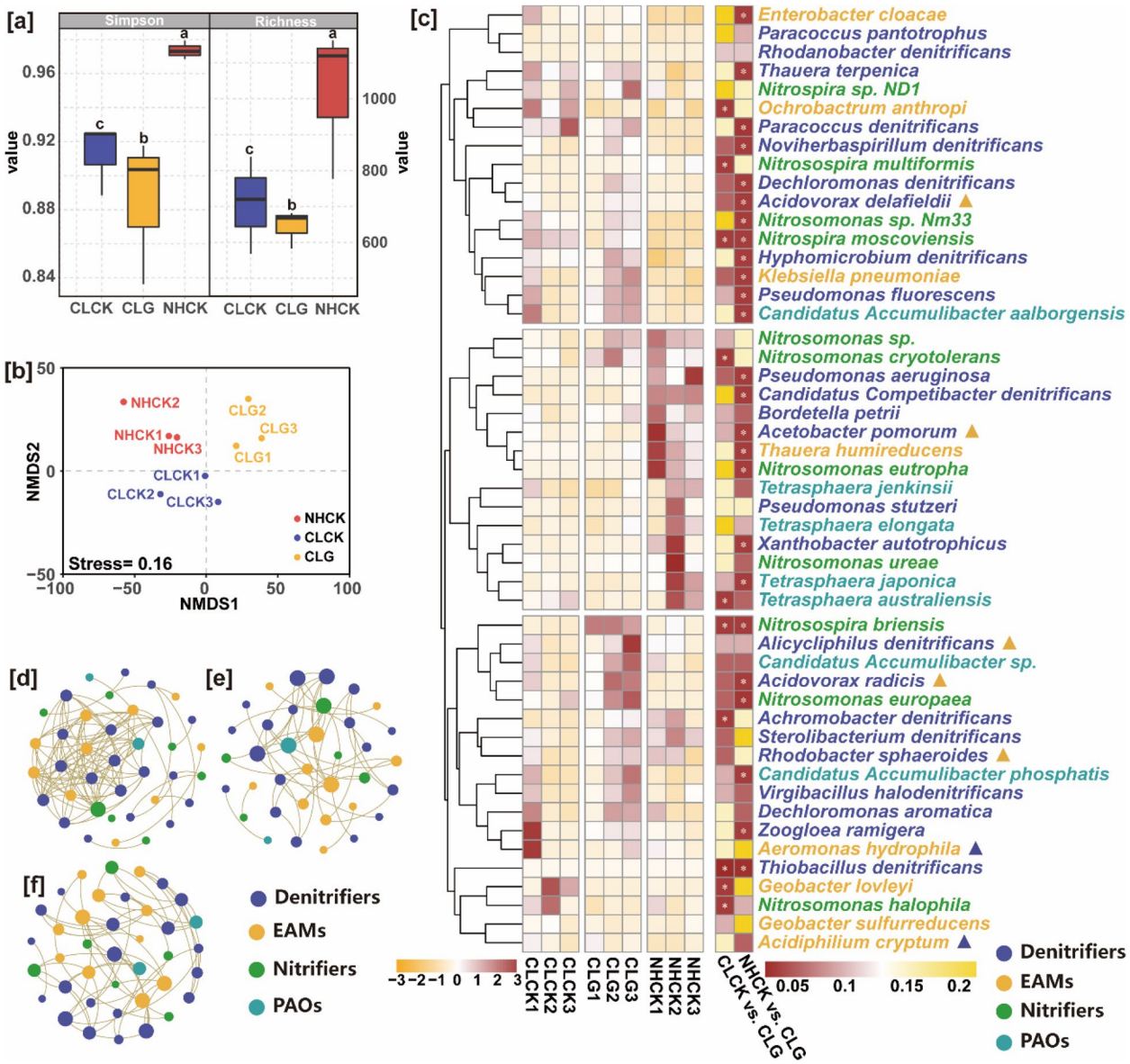

Fig. 3 Alpha-diversity of microbial community in the biofilm system in the different groups (**a**). Plots of non-metric multidimensional scaling (NMDS) analysis based on Bray–Curtis dissimilarities (**b**). Dynamics of the abundance of functional microorganisms at species level, and among them, a part of those bacteria have multi-functional traits (marked by ▲, Table S1) (**c**). Co-occurrence networks showing microbial associations in the biofilm based on the correlation analysis among functional microorganisms, including EAMs (yellow), denitrifiers (purple), nitrifiers (green), and phosphorus-accumulating microorganisms (PAO, atrovirens) (**d** NHCK, **e** CLCK, and **f** CLG). The numbers following the group names indicate the number of samples taken. The significant difference in species abundance between groups was checked by Kruskal–Wallis tests (*, $P \le 0.01$). For interpretation of the references to color in this figure legend, the reader is referred to the web version of this article

To directly assess the enrichment of EAMs and denitrifiers, changes in the abundance of known functional microorganisms were analyzed (Fig. 3c). GAC treatment effectively increased the abundance of *Klebsiella pneumoniae* under "dual-low" condition by 64.3%. *G. sulfurreducens* and *Enterobacter cloacae* showed higher abundance in GAC group, increasing with 56.4% and 76.5% respectively. *Acidiphilium cryptum* increased with 15.6% in GAC group. Other EAMs, like *G. lovleyi*, *Aeromonas hydrophila*, and *Ochrobactrum anthropi*, showed increasing trends but not significant (Fig. 3c). Notably, EAM abundance was higher under low-temperature conditions, indicating excellent low-temperature tolerance. Furthermore, the increase in denitrifiers' abundance confirmed significant enrichment in most denitrifiers with the presence of GAC in biofilm systems under "dual-low" condition (Fig. 3c). *Achromobacter denitrificans*, *Alicycliphilus denitrificans*, *Rhodobacter sphaeroides*, and *Noviherbaspirillum denitrificans* increased by 961, 286, 49, and 139 times, respectively. Larger-based denitrifiers like *Pseudomonas aeruginosa*, *Pseudomonas fluorescens*, and *Dechloromonas denitrificans* increased 63, 68, and 350 times, respectively. It is worth noting that some common denitrifiers and EAMs (*Acidiphilium cryptum*, *Acidovorax radicis*, *Alicycliphilus denitrificans*, and *Rhodobacter sphaeroides*) in GAC group simultaneously have the ability to perform extracellular electron transfer (EET) and nitrate reduction, even exceeded their abundance in biofilm system under "double-normal" conditions. Additionally, ammonia-oxidizing bacteria, short-cut nitrifying bacteria, and PAOs showed different degrees of enrichment in GAC treatment group. These results indicate that GAC presence have different enrichment effects on EAMs and denitrifiers, leading to decreased community diversity and differentiation and expansion of the microbial community structure in biofilm system.

To demonstrate the increased positive coexistence between EAMs and denitrifiers in biofilm systems, a co-occurrence analysis of identified EAMs and denitrifiers was conducted from the 16S rRNA gene profile. Results (Fig. 3d–f) showed a simpler coexistence under "dual-low" condition compared to "double-normal" condition. GAC treatment exhibited significantly increased coexistence. Coexistence relationships among nitrifiers, PAOs, and EAMs also increased. Enriching EAMs in biofilm systems links microorganisms with complementary functions through the IET process, enhancing denitrification efficiency under "dual-low" conditions.

Metatranscriptomes profiling of nitrogen and carbon metabolisms

Under "dual-low" conditions, the abundance and activity of EAMs and denitrifiers in biofilm system were enriched and enhanced, respectively. We used metatranscriptomes to detected EET gene expression, which reflected the activity of resident gram-negative EAMs (e.g., *Geobacter* spp. and *Rhodobacter* spp.) harboring evolutionarily conserved pathways. Furthermore, metatranscriptomes results quantified the transcription differences of key genes involved in microbial nitrogen metabolism and electron transfer pathways (Fig. 4). Comparing the expression differences in control and GAC groups, the results showed that the GAC treatment significantly affected the abundance of key genes involved in nitrogen metabolism and electron transfer pathways. In the denitrification process, the GAC enhancement strategies significantly upregulated the abundance of denitrifying enzyme genes, such as EC: 1.7.5.1, 1.7.2.1, 1.7.2.5, and 1.7.2.4 (Fig. 4a). Most annotated genes were both upregulated and downregulated among the treatment groups. However, the upregulated genes in denitrification were much more than the downregulated genes, consistent with increased denitrifying efficiency and decreased N_2O release. Notably, ammonia-oxidizing (EC 1.7.2.6) and nitrite-reducing (EC 1.7.2.2) enzyme genes generally showed a trend of downregulation under the GAC treatment. Nitrogen-fixing enzyme genes (EC 1.18.6.1 and 1.18.6.2) were not significantly changed in the biofilm system.

In the electron transfer pathway of gram-negative EAMs, key enzyme gene abundance varied significantly. Generally, gram-negative EAMs have two EET pathways, which are determined by key genes (e.g., *Omc* and *Mtr*) in EAMs. The "Mtr" pathway, which is generally considered to be dominated by *Shewanella* spp. [47], and the "Omc" pathway, primarily associated with *Geobacter* spp. [48]. As shown in Fig. 4b, compared to the biofilm system under "dual-low" conditions, GAC treatment upregulated genes encoding quinone pool proteins in both of two EET pathways. Rapid EET via GAC may not effectively enhance key enzyme activity. Changes in genes encoding key pigment proteins in EAMs were analyzed. *Omc*B and *Mac*A genes in "Omc" pathway significantly increased in GAC group; meanwhile, *Mtr*C/F and *Mtr*B/E genes in "Mtr" pathway were upregulated significantly (Fig. 4b). Overall, GAC mainly benefited gram-negative EAMs, which aligns with their upregulated electron transfer gene expression and observed enrichment under dual-low conditions (Fig. 3b).

Variations in denitrification and greenhouse gas reduction in biofilm system

The enhanced electron transfer efficiency and upregulated denitrification genes in GAC-biofilm systems ("Composition and function of biofilm system", "Reshaping of EAMs and denitrifiers community in

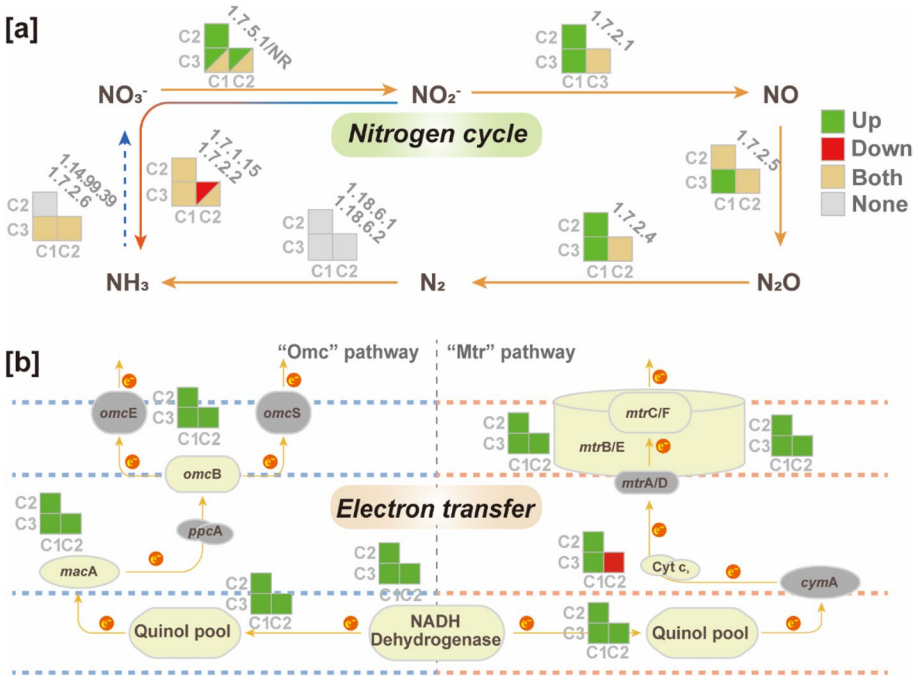

Fig. 4 **a** Abundance responses and comparison of key genes encoding enzymes in nitrogen metabolism process. **b** "Omc" and "Mtr" electron transfer pathways in different groups, which represent orthologs from dominant community gram-negative EAMs. The green boxes represent the significant upregulated abundance of key genes encoding enzymes comparing the *y*-axis to *x*-axis groups (C1 CLCK, C2 CLG, and C3 NHCK), and the red boxes are the downregulated abundance, the yellows are both up- and downregulated abundance, and the gray is the unannotated genes. The fold-change values are showed in supplementary materials (Dataset 1) for reference

biofilm" and "Metatranscriptomes profiling of nitrogen and carbon metabolisms" sections) directly improved nitrogen removal and reduced GHG emissions under "dual-low" conditions. Detailly, compared to the control (67.1% NO_3^--N removal), GAC treatment achieved 82.8% efficiency with minimal NO_2^--N accumulation (< 5 mg/L) under "dual-low" condition (Fig. 5). At normal temperature with low carbon, GAC mitigated the control's NO_3^--N reduction decline (54.4 to 67.0%) and suppressed NO_2^--N accumulation (from > 30 to < 10 mg/L). TOC removal was also significantly enhanced under low temperatures, underscoring GAC's dual role in carbon utilization and denitrification optimization (Figure S3).

GHG emissions exhibited temperature-dependent trends: GAC reduced N_2O by 10.6–22.9% under dual-low conditions, lowering global warming potential (GWP) by 8.5–15.2% (Fig. 6). However, under normal temperature, despite N_2O reductions (11.5–18.6%), GWP mitigation was limited by a twofold increase in CH_4 emissions. These results highlight GAC's efficacy in balancing nitrogen removal and GHG control under carbon- and temperature-limited regimes, while revealing trade-offs in methane dynamics under warmer conditions.

Discussion

The integration of GAC into biofilm systems under dual-low conditions represents a transformative approach to enhancing denitrification efficiency while mitigating GHG emissions. Our findings demonstrate that GAC serves as a dual-functional mediator, not only improving electron transfer between EAMs and denitrifiers but also reshaping microbial community dynamics to favor functional synergies. This study advances the mechanistic understanding of IET and provides actionable insights for optimizing biofilm-based wastewater treatment systems in challenging environments. Below, we contextualize these results within broader scientific and environmental frameworks, addressing both mechanistic innovations and practical implications.

Mechanistic insights into GAC-mediated electron transfer

The observed 19.4–21.9% improvement in denitrification efficiency under "dual-low" conditions (Fig. 5) aligns with GAC's role as an electron mediator. GAC's porous structure provides a high surface area for microbial colonization and facilitates direct-IET by acting as a conductive bridge between EAMs and denitrifiers (Fig. 4c). This mechanism is supported by SEM and FISH analyses,

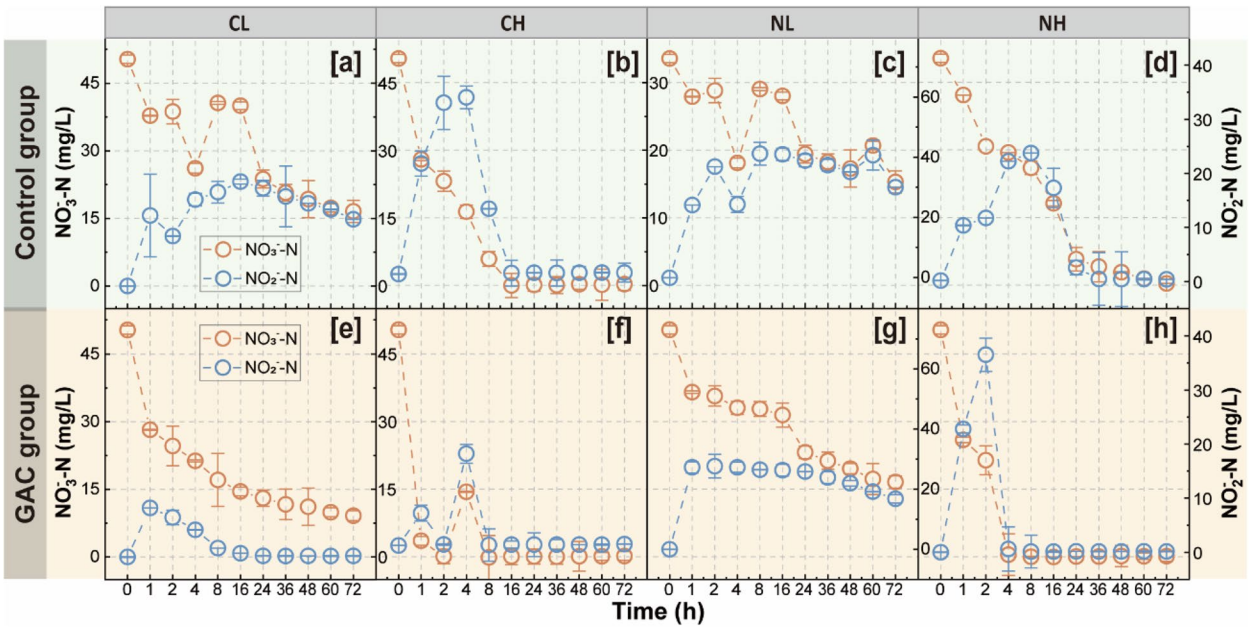

Fig. 5 Denitrification responses of nitrate (blue) and nitrite (orange) in the biofilm system along with time. CL, low temperature (4–6°C) and low carbon source (C/N = 4) (**a** and **e**). CH, low temperature (4–6°C) and normal carbon source (C/N = 8) (**b** and **f**). NL, normal temperature (25 ± 1°C) and low carbon source (C/N = 4) (**c** and **g**). NH, normal temperature (25 ± 1°C) and normal carbon source (C/N = 8) (**d** and **h**). Error bars mean the standard deviation ($n = 3$)

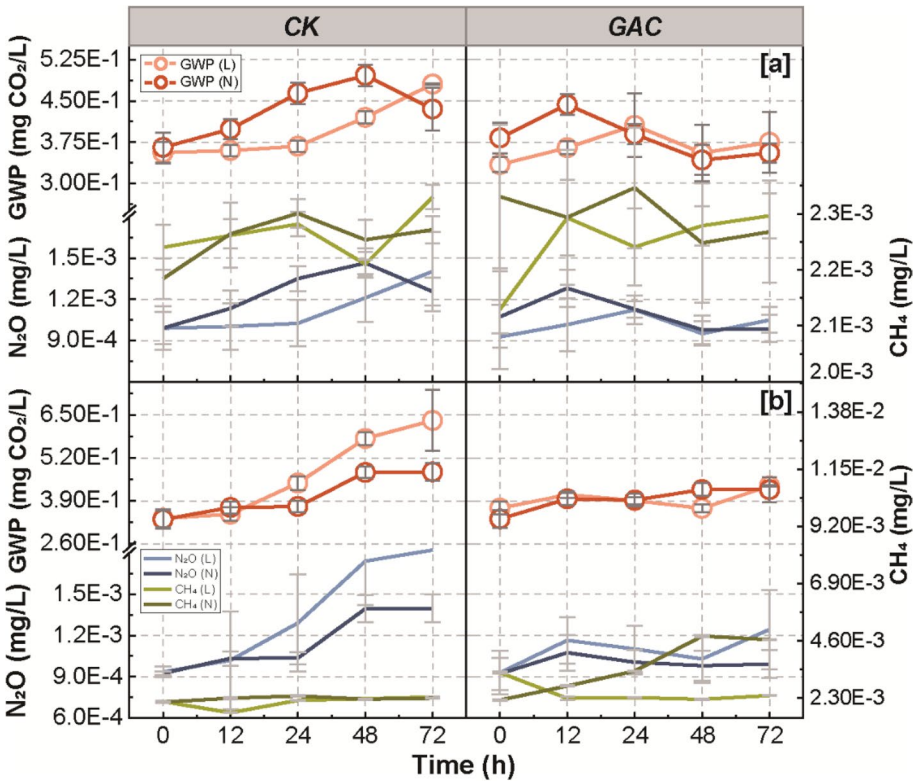

Fig. 6 Greenhouse gas (nitrous oxide and methane) emission and global warming potential (GWP) responses in the biofilm system along with time. **a** Low temperature (4–6°C). **b** Normal temperature (25 ± 1°C). The letters of "L" and "N" indicate "low" and "normal" carbon source. Error bars mean the standard deviation ($n = 3$)

which revealed nanowire-like structures connecting *Geobacter* spp. (EAMs) and *Pseudomonas* spp. (denitrifiers) (Fig. 1). Such physical linkages enable efficient electron shuttling, bypassing the need for soluble redox shuttles like flavins or quinones, which is less effective under low-carbon conditions [26, 33]. The upregulation of key electron transport genes (Fig. 4b) further corroborated GAC's ability to enhance EET pathways ("Omc" or "Mtr" pathway). Notably, GAC treatment preferentially enriched cold-adapted gram-negative EAMs (e.g., *Geobacter sulfurreducens*), likely due to their conductive pili and outer-membrane cytochrome networks that facilitate extracellular electron transfer under low-temperature stress [22, 38]. Beyond structural visualization, we addressed the limitation of 2D imaging by employing in situ biofilm potential mapping using Th.T staining. As shown in Fig. 2b, the GAC-enhanced biofilms exhibited stronger and spatially continuous Th.T signals, indicating higher membrane potential and more extensive electron flux. Together with the system-wide increases in ETE and ATP (Fig. 2a), and the transcriptional upregulation of electron transfer genes, these results demonstrate that GAC fosters not only spatial co-aggregation but also functional electrochemical connectivity across the biofilm matrix.

The formation of EAM-denitrifier coacervates (Fig. 1d) suggests a novel symbiotic relationship driven by electrochemical gradients. These microenvironments create localized redox niches where EAMs oxidize residual organic carbon, while denitrifiers utilize electrons from GAC or EAMs to reduce nitrate. This spatial organization minimizes electron loss and reduces intermediate accumulation (e.g., NO_2^-; Fig. 5), thereby lowering N_2O emissions by 10.6–22.9% (Fig. 6). Similar direct-IET-driven partnerships have been reported in anaerobic digesters [49] and co-culture system [50], but our study uniquely demonstrates their applicability to low-temperature biofilm systems, expanding the scope of direct-IET applications.

Ecological and functional implications of microbial community reshaping

The integration of GAC significantly restructured the microbial ecology of the biofilm system under dual-low conditions, favoring the emergence of a functionally specialized consortium enriched in EAMs and denitrifiers. Metatranscriptome analyses revealed that this restructuring was not merely compositional but deeply functional, with pronounced upregulation of genes involved in EET and denitrification pathways.

Under GAC treatment, keystone species such as *Geobacter sulfurreducens* and *Pseudomonas fluorescens* dominated the biofilm community. The ecological relevance of their enrichment lies in their metabolic complementarities: *G. sulfurreducens* actively expresses genes in the "Omc" pathway (e.g., *omc*B and *mac*A) for efficient electron donation, while *P. fluorescens* upregulates *nos*Z, facilitating the final reduction of NO_3^--N to N_2, thereby closing the denitrification loop and mitigating greenhouse gas emissions. These synergistic interactions are substantiated by metatranscriptomes data showing simultaneous activation of electron transfer genes and nitrate reduction enzymes, indicating spatial and functional coupling of metabolic roles.

Interestingly, while alpha-diversity declined under GAC treatment (Fig. 3a), co-occurrence networks (Fig. 3d–f) became denser and more functionally coherent. This suggests a shift from a broadly diverse but loosely interacting community to a tightly linked and functionally redundant microbial consortium [46]. For example, *Acidiphilium cryptum* and *Alicycliphilus denitrificans* not only contributed to nitrate reduction but also expressed EET-related genes, reflecting dual-function traits that bridge traditional ecological guilds. Such redundancy in critical functions like denitrification and EET enhances system resilience under stress, such as low temperature and limited carbon [22].

The network analysis further revealed increased interconnectivity between EAMs, denitrifiers, nitrifiers, and PAOs. This tripartite synergy may facilitate nutrient cycling beyond nitrogen. Specifically, PAOs may scavenge carbon substrates released by EAMs, stabilizing carbon flow and indirectly supporting denitrifier activity. This emergent metabolic network, enabled by GAC, represents a form of engineered microbial cooperation wherein conductive materials serve as ecological scaffolds for community assembly and functional alignment.

Another key observation from metatranscriptomes data is the differential expression of EET pathways (Fig. 4). Genes in the "Mtr" pathway (e.g., *mtr*C, *mtr*F) were upregulated, and the presence of "Mtr"-pathway EAMs cannot be neglected in 16S rRNA datasets. This raises two ecological possibilities: (i) rare taxa may contribute disproportionately to functional output through high gene expression per biomass, or (ii) horizontal gene transfer or convergent functional pathways may allow "Mtr" pathway taxa to perform Mtr-like electron transport. This targeted enrichment strategy favored gram-negative keystone taxa with strong EET capabilities and cold tolerance, including *Geobacter sulfurreducens*, *Acidovorax radices*, and *Alicycliphilus denitrificans*. In either case, the data highlight the importance of functional rather than taxonomic resolution in interpreting microbial ecology under engineered perturbations.

Taken together, GAC-induced microbial restructuring exemplifies a targeted ecological engineering strategy.

By enriching microbial taxa with high EET capacity and denitrification potential, GAC not only accelerates biogeochemical cycling but also creates electrochemically active microenvironments conducive to stable and efficient nitrogen removal. These findings underscore that engineered biofilm systems, when informed by microbial ecological principles and validated via metatranscriptomes, can serve as adaptive platforms for sustainable wastewater treatment. Future studies should expand on these ecological interactions using isotope labeling or single-cell transcriptomics to trace interspecies electron flow and metabolic exchange. Such efforts will deepen our understanding of how conductive materials mediate ecological network formation and stabilize ecosystem services under environmental constraints.

Practical challenges and scalability

While laboratory-scale results are promising, translating GAC-based strategies to full-scale WWTPs requires addressing several challenges. First, GAC's long-term stability under continuous flow conditions remains untested. Biofouling or abrasion in large reactors could diminish its electron-mediating capacity over time. Second, the economic feasibility of GAC integration must be evaluated. Although GAC is commercially available, its cost compared to conventional carriers (e.g., ceramsite) and the energy savings from reduced GHG emissions need thorough lifecycle assessment [51]. Pilot-scale trials integrating GAC with existing biofilm reactors (e.g., moving bed biofilm reactors, MBBRs) could provide critical data on operational durability and cost-effectiveness.

Moreover, the interplay between GAC and real wastewater matrices—which contain complex organics, toxins, and fluctuating nutrient loads—may alter microbial interactions. For example, humic substances in wastewater could compete with GAC as electron shuttles, potentially diminishing its efficacy [32]. Future studies should explore GAC's performance in diverse wastewater types and its compatibility with tertiary treatment processes (e.g., membrane filtration).

Global climate impact and alignment with SDGs

The reduction in N_2O emissions achieved here holds significant implications for climate change mitigation. N_2O is a potent GHG with 265 times the global warming potential of CO_2 over a 100-year horizon [4]. By curbing N_2O release by 10.6–22.9%, GAC-amended biofilm systems directly contribute to SDG 13 (Climate Action). Furthermore, improved nitrogen removal efficiency supports SDG 6 (Clean Water) by reducing nitrate discharge into aquatic ecosystems, thereby mitigating eutrophication and protecting biodiversity.

The integration of GAC into biofilm systems also aligns with the "carbon neutrality" agenda. Traditional denitrification processes often require external carbon supplementation (e.g., methanol), which increases operational costs and carbon footprints [8]. GAC's ability to enhance endogenous carbon utilization (evidenced by higher TOC removal under low temperatures; Figure S3) reduces reliance on exogenous carbon sources, lowering both economic and environmental burdens. This dual benefit positions GAC as a sustainable alternative to carbon-intensive treatment methods.

Limitation analysis

Our study acknowledges methodological limitations and analytical constraints. First, while SEM imaging alone cannot definitively attribute nanowire connections to specific taxa, we employed dual-probe FISH targeting electroactive microorganisms (EAMs) and denitrifiers. Confocal imaging revealed spatially close coaggregates, with EAMs frequently encasing denitrifiers—an arrangement consistent with chemotactic electron donor-recipient enrichment. This spatial architecture, combined with SEM-observed filamentous structures, supports GAC-induced direct interspecies electron transfer (DIET). Second, although correlation analyses cannot establish causality, we addressed this limitation through integrated experimental approaches. Metatranscriptomes data demonstrated that GAC treatment under dual-low conditions significantly upregulated genes for extracellular electron transport (*omc*B, *mtr*C, *mac*A in *Geobacter*/*Shewanella*) and denitrification (*nos*Z), directly linking EAM and denitrifier activity. This functional evidence transcends taxonomic correlation and provides mechanistic insight into DIET. Third, while elevated ATP and ETE reflect enhanced overall microbial activity, the targeted enrichment of key EAMs (e.g., *Geobacter sulfurreducens*) and denitrifiers (e.g., *Pseudomonas fluorescens*), coupled with their functional gene expression, strongly indicates GAC-facilitated metabolic cooperation. Distinct shifts in microbial composition and co-occurrence networks under GAC further suggest reorganization favoring DIET partnerships. Finally, observed gains in denitrification efficiency (up to 21.9%) and concurrent N_2O emission reduction under GAC treatment, without exogenous carbon, imply a shift towards more efficient electron sharing between EAMs and denitrifiers, consistent with DIET. We concur that those future techniques (e.g., isotope probing, real-time electrochemical tracking) could offer more direct validation; nevertheless, our integrated multi-omics, imaging, and functional data robustly support that GAC enhanced interspecies electron transfer, significantly contributing to improved denitrification under dual-low conditions.

Although our current study employs multi-omics analysis, FISH-SEM imaging, and functional assays to demonstrate that granular activated carbon (GAC) promotes the enrichment and co-localization of electroactive microorganisms (EAMs) and denitrifiers, we acknowledge that these indirect approaches cannot fully resolve the underlying electron transfer mechanisms. Future work should involve co-culture experiments using model strains (e.g., representative exoelectrogens and denitrifiers) enriched from the GAC-amplified system in dual-chamber microbial fuel cells (MFCs). This setup would allow precise tracking of electron flow under controlled conditions, direct assessment of GAC's impact on nitrate reduction efficiency and denitrification gene expression, and simultaneous real-time monitoring of current production and nitrogen removal, thereby directly validating the EET pathways involved.

Future directions and innovations

To maximize the potential of GAC-mediated systems, interdisciplinary approaches are needed:

- Material engineering: Developing GAC composites with embedded catalysts (e.g., Fe^{3+}, Cu^{2+}) could further accelerate electron transfer. Metal-doped GAC has shown promise in enhancing DIET in anaerobic digestion [52], and similar strategies could be adapted for biofilm systems.
- Microbial engineering: Enriching biofilms with genetically engineered EAMs or denitrifiers—optimized for low-temperature activity or enhanced EET—could push performance boundaries. For example, *Shewanella oneidensis* engineered with overexpressed *mtr*CAB pathways exhibits superior electron transfer rates [24].
- System hybridization: Coupling GAC-amended biofilms with emerging technologies like microbial electrochemical systems (MES) or phototrophic biofilms could create self-sustaining treatment systems. MES, for instance, could harvest electrons from EAMs to generate renewable energy while driving denitrification [18].

Conclusion

This study elucidates the pivotal role of GAC in overcoming the intrinsic limitations of biofilm systems under "dual-low" conditions. By fostering DIET, reshaping microbial consortia, and mitigating GHG emissions, GAC emerges as a versatile tool for sustainable wastewater management. While challenges in scalability and real-world application persist, the environmental and economic benefits demonstrated here provide a compelling rationale for further research and pilot-scale validation. As global efforts to achieve SDGs intensify, innovations like GAC-mediated biofilm systems will be critical in bridging the gap between wastewater treatment efficiency and planetary health.

Supplementary Information

The online version contains supplementary material available at https://doi.org/10.1186/s40168-025-02161-3.

Supplementary Material 1.

Supplementary Material 2.

Acknowledgements
We thank Shanghai Major Biotechnology Co., Ltd. for bioinformatics analysis and data processing.

Authors' contributions
X.Y.: study design, performing experiments, data analysis, and manuscript writing. M.Y., L.Z., and P.L.: performing experiments, and data analysis. J.P.H. and G.L.: study design, data interpretation, and overall supervision.

Funding
Supported in part by grants 52261145702 (G.L.) and 52200077 (X.Y.) from the National Natural Science Foundation of China; Postdoctoral Fellowship Program (Grade B) of China Postdoctoral Science Foundation No. GZB20230691 (X.Y.); Shandong Excellent Young Scientists Fund Program (Overseas) No. 2024HWYQ-040 (X.Y.); and Taishan Scholars Young Expert Program No. tsqn202408074 (X.Y.).

Data availability
Sequence data of 16S rRNA gene and metatransgenomic that support the findings of this study have been deposited in the NCBI Sequence Read Archive (SRA) under the accession number PRJNA995884.

Declarations

Ethics approval and consent to participate
Not applicable.

Consent for publication
Not applicable.

Competing interests
The authors declare no competing interests.

Received: 30 March 2025 Accepted: 9 June 2025
Published online: 01 August 2025

References

1. Erisman JW, Sutton MA, Galloway J, Klimont Z, Winiwarter W. How a century of ammonia synthesis changed the world. Nat Geosci. 2008;1(10):636–9.
2. Erisman JW, Galloway JN, Seitzinger S, Bleeker A, Dise NB, Petrescu AMR, Leach AM, de Vries W. Consequences of human modification of the global nitrogen cycle. Philos Trans R Soc Lond B Biol Sci. 2013;368(1621):20130116.
3. Galloway JN, Townsend AR, Erisman JW, Bekunda M, Cai Z, Freney JR, Martinelli LA, Seitzinger SP, Sutton MA. Transformation of the nitrogen cycle: recent trends, questions, and potential solutions. Science. 2008;320(5878):889–92.
4. Harris E, Yu L, Wang YP, Mohn J, Henne S, Bai E, Barthel M, Bauters M, Boeckx P, Dorich C, Farrell M, Krummel PB, Loh ZM, Reichstein M, Six J, Steinbacher M, Wells NS, Bahn M, Rayner P. Warming and redistribution

of nitrogen inputs drive an increase in terrestrial nitrous oxide emission factor. Nat Commun. 2022;13(1):4310.
5. Morseletto P. Confronting the nitrogen challenge: options for governance and target setting. Glob Environ Change-Human Policy Dimensions. 2019;54:40–9.
6. Sutton MA, Howard CM, Kanter DR, Lassaletta L, Moring A, Raghuram N, Read N. The nitrogen decade: mobilizing global action on nitrogen to 2030 and beyond. One Earth. 2021;4(1):10–4.
7. Cullen L, Meng F, Lupton R, Cullen JM. Reducing uncertainties in greenhouse gas emissions from chemical production. Nat Chem Eng. 2024;1(4):311–22.
8. Scown CD. The short- and long-run environmental value of waste conversion. Nat Chem Eng. 2024;1(5):326–326.
9. Kehrein P, van Loosdrecht M, Osseweijer P, Garfi M, Dewulf J, Posada J. A critical review of resource recovery from municipal wastewater treatment plants - market supply potentials, technologies and bottlenecks. Environ Sci-Water Res Technol. 2020;6(4):877–910.
10. Kumar A, Thanki A, Padhiyar H, Singh NK, Pandey S, Yadav M, Yu Z-G. Greenhouse gases emission control in WWTS via potential operational strategies: a critical review. Chemosphere. 2021;273:129694.
11. Shama S, Iffat N. Role of the biofilms in wastewater treatment. Microbial Biofilms. 2016;10:63499.
12. Chen X, Yang L, Sun J, Wei W, Liu Y, Ni B-J. Influences of longitudinal heterogeneity on nitrous oxide production from membrane-aerated biofilm reactor: a modeling perspective. Environ Sci Technol. 2020;54(17):10964–73.
13. Uri-Carren N, Nielsen PH, Gernaey KV, Domingo-Felez C, Flores-Alsina X. Nitrous oxide emissions from two full-scale membrane-aerated biofilm reactors. Sci Total Environ. 2024;908:168030.
14. Walden C, Zhang W. Biofilms versus activated sludge: considerations in metal and metal oxide nanoparticle removal from wastewater. Environ Sci Technol. 2016;50(16):8417–31.
15. Daigger GT, Kuo J, Derlon N, Houweling D, Jimenez JA, Johnson BR, McQuarrie JP, Murthy S, Regmi P, Roche C, Sturm B, Wett B, Winkler M, Boltz JP. Biological and physical selectors for mobile biofilms, aerobic granules, and densified-biological flocs in continuously flowing wastewater treatment processes: a state-of-the-art review. Water Res. 2023;242:120245.
16. Philipp L-A, Buehler K, Ulber R, Gescher J. Beneficial applications of biofilms. Nat Rev Microbiol. 2024;22(5):276–90.
17. Leventhal GE, Boix C, Kuechler U, Enke TN, Sliwerska E, Holliger C, Cordero OX. Strain-level diversity drives alternative community types in millimetre-scale granular biofilms. Nat Microbiol. 2018;3(11):1295–303.
18. Doherty L, Zhao Y, Zhao X, Hu Y, Hao X, Xu L, Liu R. A review of a recently emerged technology: constructed wetland - microbial fuel cells. Water Res. 2015;85:38–45.
19. Aguirre-Sierra A, Bacchetti-De GT, Salas JJ, de Deus A, Esteve-Núñez A. A new concept in constructed wetlands: assessment of aerobic electroconductive biofilters. Environ Sci-Water Res Technol\. 2020;6(5):1312–23.
20. Lu L, Xing DF, Ren ZJ. Microbial community structure accompanied with electricity production in a constructed wetland plant microbial fuel cell. Biores Technol. 2015;195:115–21.
21. Kato S, Hashimoto K, Watanabe K. Microbial interspecies electron transfer via electric currents through conductive minerals. Proc Natl Acad Sci USA. 2012;109(25):10042–6.
22. Larrosa-Guerrero A, Scott K, Head IM, Mateo F, Ginesta A, Godinez C. Effect of temperature on the performance of microbial fuel cells. Fuel. 2010;89(12):3985–94.
23. Tkach O, Sangeetha T, Maria S, Wang AJ. Performance of low temperature Microbial Fuel Cells (MFCs) catalyzed by mixed bacterial consortia. J Environ Sci. 2017;52:284–92.
24. Marsili E, Baron DB, Shikhare ID, Coursolle D, Gralnick JA, Bond DR. Shewanella Secretes flavins that mediate extracellular electron transfer. Proc Natl Acad Sci USA. 2008;105(10):3968–73.
25. Brutinel ED, Gralnick JA. Shuttling happens: soluble flavin mediators of extracellular electron transfer in Shewanella. Appl Microbiol Biotechnol. 2012;93(1):41–8.
26. Liu FH, Rotaru AE, Shrestha PM, Malvankar NS, Nevin KP, Lovley DR. Promoting direct interspecies electron transfer with activated carbon. Energy Environ Sci. 2012;5(10):8982–9.
27. Wolf M, Kappler A, Jiang J, Meckenstock RU. Effects of humic substances and quinones at low concentrations on ferrihydrite reduction by *Geobacter metallireducens*. Environ Sci Technol. 2009;43(15):5679–85.
28. Straub KL, Kappler A, Schink B. Enrichment and isolation of ferric-iron- and humic-acid-reducing bacteria. Environ Microbiol. 2005;397:58–77.
29. Yan XJ, Du Q, Mu QH, Tian LL, Wan YX, Liao CM, Zhou LA, Yan YQ, Li N, Logan BE, Wang X. Long-term succession shows interspecies competition of geobacter in exoelectrogenic biofilms. Environ Sci Technol. 2021;55(21):14928–37.
30. Yang YG, Xu MY, Guo J, Sun GP. Bacterial extracellular electron transfer in bioelectrochemical systems. Process Biochem. 2012;47(12):1707–14.
31. Scott DT, McKnight DM, Blunt-Harris EL, Kolesar SE, Lovley DR. Quinone moieties act as electron acceptors in the reduction of humic substances by humics-reducing microorganisms. Environ Sci Technol. 1998;32(19):2984–9.
32. Walpen N, Getzinger GJ, Schroth MH, Sander M. Electron-donating phenolic and electron-accepting quinone moieties in peat dissolved organic matter: quantities and redox transformations in the context of peat biogeochemistry. Environ Sci Technol. 2018;52(9):5236–45.
33. Guo F, Luo Y, Nie W, Xiong Z, Yang X, Yan J, Liu T, Chen M, Chen Y. Biochar boosts nitrate removal in constructed wetlands for secondary effluent treatment: linking nitrate removal to the metabolic pathway of denitrification and biochar properties. Biores Technol. 2023;379:129000.
34. Su X, Wen T, Wang Y, Xu J, Cui L, Zhang J, Xue X, Ding K, Tang Y, Zhu Y-G. Stimulation of N_2O emission via bacterial denitrification driven by acidification in estuarine sediments. Glob Change Biol. 2021;27(21):5564–79.
35. Liu X, Yang X, Hu X, He Q, Zhai J, Chen Y, Xiong Q, Vymazal J. Comprehensive metagenomic analysis reveals the effects of silver nanoparticles on nitrogen transformation in constructed wetlands. Chem Eng J. 2019;358:1552–60.
36. Yang X, Chen Y, Guo F, Liu X, Su X, He Q. Metagenomic analysis of the biotoxicity of titanium dioxide nanoparticles to microbial nitrogen transformation in constructed wetlands. J Hazard Mater. 2020;384:121376.
37. Roots P, Wang Y, Rosenthal AF, Griffin JS, Sabba F, Petrovich M, Yang F, Kozak JA, Zhang H, Wells GF. Comammox Nitrospira are the dominant ammonia oxidizers in a mainstream low dissolved oxygen nitrification reactor. Water Res. 2019;157:396–405.
38. Liu X, Zhuo S, Rensing C, Zhou S. Syntrophic growth with direct interspecies electron transfer between pili-free *Geobacter* species. ISME J. 2018;12(9):2142–51.
39. McIlroy SJ, Starnawska A, Starnawski P, Saunders AM, Nierychlo M, Nielsen PH, Nielsen JL. Identification of active denitrifiers in full-scale nutrient removal wastewater treatment systems. Environ Microbiol. 2016;18(1):50–64.
40. Yao MC, Zhang Y, Dai ZH, Ren AR, Fang JX, Li XM, van der Meer W, Medema G, Rose JB, Liu G. Building water quality deterioration during water supply restoration after interruption: influences of premise plumbing configuration. Water Res. 2023;241:120149.
41. Yang X, He Q, Guo F, Sun X, Zhang J, Chen M, Vymazal J, Chen Y. Nanoplastics disturb nitrogen removal in constructed wetlands: responses of microbes and macrophytes. Environ Sci Technol. 2020;54(21):14007–16.
42. Broberg A. A modified method for studies of electron-transport system activity in fresh-water sediments. Hydrobiologia. 1985;120(2):181–7.
43. Prindle A, Liu J, Asally M, Ly S, Garcia-Ojalvo J, Sueel GM. Ion channels enable electrical communication in bacterial communities. Nature. 2015;527(7576):59–63.
44. Yang X, He Q, Liu T, Zheng F, Mei H, Chen M, Liu G, Vymazal J, Chen Y. Impact of microplastics on the treatment performance of constructed wetlands: based on substrate characteristics and microbial activities. Water Res. 2022;217:118430.
45. Yang X, Zhang L, Chen Y, He Q, Liu T, Zhang G, Yuan L, Peng H, Wang H, Ju F. Micro(nano)plastic size and concentration co-differentiate nitrogen transformation, microbiota dynamics, and assembly patterns in constructed wetlands. Water Res. 2022;220:118636–118636.
46. Ju F, Lau F, Zhang T. Linking microbial community, environmental variables, and methanogenesis in anaerobic biogas digesters of chemically enhanced primary treatment sludge. Environ Sci Technol. 2017;51(7):3982–92.
47. Kouzuma A, Kasai T, Hirose A, Watanabe K. Catabolic and regulatory systems in Shewanella oneidensis MR-1 involved in electricity generation in microbial fuel cells. Front Microbiol. 2015;6:609.

48. Liu Y, Wang Z, Liu J, Levar C, Edwards MJ, Babauta JT, Kennedy DW, Shi Z, Beyenal H, Bond DR, Clarke TA, Butt JN, Richardson DJ, Rosso KM, Zachara JM, Fredrickson JK, Shi L. A trans-outer membrane porin-cytochrome protein complex for extracellular electron transfer by Geobacter sulfurreducens PCA. Environ Microbiol Rep. 2014;6(6):776–85.
49. Zheng S, Liu F, Wang B, Zhang Y, Lovley DR. Methanobacterium capable of direct interspecies electron transfer. Environ Sci Technol. 2020;54(23):15347–54.
50. Yang XY, Yao MC, Li P, van der Hoek JP, Zhang LJ, Liu G. Mutual symbiosis of electroactive bacteria and denitrifiers for improved refractory carbon utilization and nitrate reduction. Environ Int. 2025;197:10.
51. Ellis AC, Boyer TH, Fang Y, Liu CJ, Strathmann TJ. Life cycle assessment and life cycle cost analysis of anion exchange and granular activated carbon systems for remediation of groundwater contaminated by per- and polyfluoroalkyl substances (PFASs). Water Res. 2023;243:120324.
52. Wang ZX, Wang TF, Si BC, Watson J, Zhang YH. Accelerating anaerobic digestion for methane production: potential role of direct interspecies electron transfer. Renew Sustain Energy Rev. 2021;145:111069.

Publisher's Note